

Electron fishbones: theory and experimental evidence

F. Zonca 1), P. Buratti 1), A. Cardinali 1), L. Chen 2), J.-Q. Dong 3), Y.-X. Long 4), A. Milovanov 1)-5)-6), F. Romanelli 1), P. Smeulders 1), L. Wang 3) and Z.-T. Wang 3)

1) Associazione Euratom-ENEA sulla Fusione, C.P. 65 - I-00044 - Frascati, Rome, Italy

2) Dept. of Physics and Astronomy, Univ. of California, Irvine CA 92697-4575, U.S.A.

3) Southwestern Institute of Physics, P.O. Box 432, Chengdu 610041, P.R.C.

4) Institute of Physics, Chinese Academy of Sciences, Beijing 100080, P.R.C.

5) Department of Physics and Technology, University of Tromsø, N-9037 Tromsø, Norway

6) Space Research Institute, Russian Academy of Sciences, Moscow, Russia

e-mail contact of main author: zonca@frascati.enea.it

Abstract. We discuss the processes underlying the excitation of fishbone-like internal kink instabilities driven by supra-thermal electrons generated experimentally by different means: Electron Cyclotron Resonance Heating (ECRH) and by Lower Hybrid (LH) power injection. The peculiarity and interest of exciting these electron fishbones by ECRH only or by LH only is also analyzed. Not only the mode stability is explained, but also the transition between steady state nonlinear oscillations to bursting (almost regular) pulsations, as observed in FTU, is interpreted in terms of the LH power input. These results are directly relevant to the investigation of trapped alpha particle interactions with low-frequency MHD modes in burning plasmas: in fact, alpha particles in reactor relevant conditions are characterized by small dimensionless orbits, similarly to electrons; the trapped particle bounce averaged dynamics, meanwhile, depends on energy and not mass.

1. Introduction and Background

Fishbone - like internal kink instabilities driven by electrons have been observed for the first time on DIII-D in conjunction with Electron Cyclotron Resonance Heating (ECRH) on the high field side [1]. There, the excitation was attributed to *barely trapped supra-thermal electrons*, which are characterized by *drift-reversal* and can destabilize a mode propagating in the ion diamagnetic direction in the presence of an *inverted spatial gradient* of the supra-thermal tail. Similar but higher frequency modes were observed in Compass-D [2] during ECRH and Lower Hybrid (LH) power injection, with *chirping* frequency comparable with that of the Toroidal Alfvén Eigenmode [3] (TAE), $\omega \lesssim \omega_{TAE}$. Observations of *electron fishbones* with ECRH only [4, 5] and LH only [6, 7] have been also reported in HL-1M and FTU, respectively.

In the present work, we analyze the peculiar features of electron fishbones versus those of the well known ion fishbone [8, 9, 10]. Due to the frequency gap in the low-frequency shear Alfvén continuum for modes propagating in the ion diamagnetic direction [10], effective electron fishbone excitation favors conditions characterized by supra-thermal electron drift reversal, consistently with experimental observations. For the same reason, the spatial gradient inversion of the supra-thermal electron tail is necessary, explaining why ECRH excitation is observed with high field side deposition only [1, 4, 5, 11]. Here, we also discuss the peculiar roles of *circulating supra-thermal electrons* for electron fishbone excitations with LH only: the *barely circulating* population providing directly the mode drive and the *well circulating* particles controlling the drift-reversal condition. As in the case of ion fishbones, two branches of the electron fishbone are shown to exist: a discrete gap mode [10] and a continuum resonant mode [9]. Contrary to the gap mode, the continuum resonant mode can propagate in the electron diamagnetic direction as well. Thus, it does not require neither drift-reversal nor inverted spatial gradient of

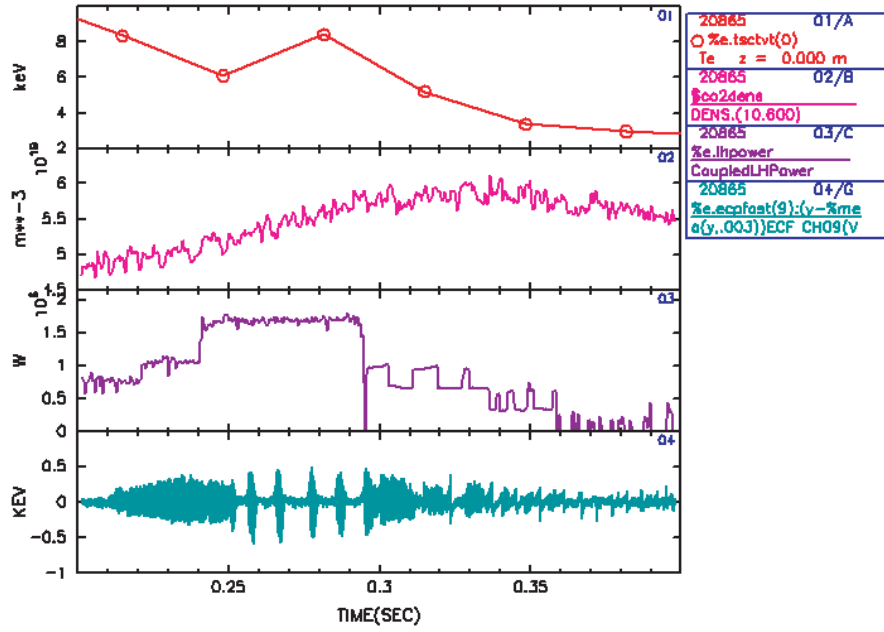


FIG. 1. Time evolution of thermal electron temperature (01), electron density (02), LH power input (03) and (fast) electron temperature fluctuation (04) in FTU shot # 20865. It is clear that the nonlinear behavior of electron temperature fluctuations (electron fishbone) reflects the level of LH power input.

the supra-thermal electron tail. However, its threshold condition is higher and it requires high power densities to be excited. Here, we discuss one single general *fishbone-like* dispersion relation [12], describing mode excitation by trapped as well as circulating supra-thermal electrons in both monotonic and reversed magnetic shear equilibria [13].

In this work, we also analyze the nonlinear physics of electron fishbones, of which FTU experimental results provide a nice and clear example (see Figure 1): during high power LH injection, an evident transition in the electron fishbone signature takes place from almost steady state nonlinear oscillations (fixed point) to regular bursting behavior (limit cycle). Here, we present a simple yet relevant nonlinear dynamic model for predicting and interpreting these observations.

2. Mode dispersion relations

The fishbone dispersion relation can be obtained by the standard matching procedure of mode structures in the ideal region and inertial layer [14] and generalizing the results therein. Here, we choose to solve quasi-neutrality and vorticity equations following the procedure of Ref. [15], where the solution of the kinetic layer equations in the Fourier space are matched to the ideal region. Letting $x = (r - r_s)/r_s$, with r_s the radius of the $q(r_s) = 1$ surface, we introduce the representation $\delta\phi(x) = \int d\eta e^{-i\eta x} \delta\Phi(\eta)$ for the scalar potential fluctuation and other fields. For finite shear, $s = r_s q'_s/q_s$, the asymptotic ideal region solution when approaching the inertial layer is [15]

$$|\eta|\delta\Phi \simeq (\eta/|\eta|) \left(1 + |\eta|\delta\hat{W}/s^2\right), \quad (1)$$

for $1 \ll |\eta| \ll |\gamma/\omega|^{-1}$, with γ/ω the normalized mode growth rate and $\delta\hat{W}$ the normalized potential energy. Meanwhile, the inertial (kinetic) layer solution is [12]

$$|\eta|\delta\Phi \simeq (\eta/|\eta|) (1 + i|\eta|\Lambda/|s|). \quad (2)$$

Here, Λ a generalized inertia term, introduced in [12]. For the present scope, we need an explicit expression of Λ for two limiting cases: (i) the banana regime, $|\omega| \ll \omega_{bi} \ll \omega_{ti}$, with $\omega_{bi}(\omega_{ti})$ the thermal ion bounce(transit) frequency, where [16, 17]

$$\Lambda^2 = \left(\omega^2/\omega_A^2\right) (1 - \omega_{*pi}/\omega) \left[1 + \left(1.6(R_0/r)^{1/2} + 0.5\right) q^2\right] ; \quad (3)$$

(ii) the high frequency regime, $|\omega| \gg \omega_{ti}$, where [18]

$$\Lambda^2 = \frac{\omega^2}{\omega_A^2} - \frac{\omega_{BAE}^2}{\omega_A^2} \left[1 + \frac{\omega_{BAE}^2 (46/49) + (32/49)(T_e/T_i) + (8/49)(T_e/T_i)^2}{q^2 \omega^2 (1 + (4/7)(T_e/T_i))^2}\right] . \quad (4)$$

Here, $\omega_A = v_A/(qR_0)$, v_A is the Alfvén speed, $\omega_{*pi} = \mathbf{k} \times \mathbf{B}/B \cdot \nabla P_i/(n_i m_i \omega_{ci})$, \mathbf{k} is the wave-vector, $\omega_{BAE} = q\omega_{ti}(7/4 + T_e/T_i)^{1/2}$ and $\omega_{ti} = (2T_i/m_i)^{1/2}/(qR_0)$. The correct form of the enhancement factor $\propto q^2$ in Eq. (3) was first pointed out in [17]: the $1.6(R_0/r)^{1/2}q^2$ factor comes from trapped and barely circulating particles; the $0.5q^2$ term, meanwhile, is due to well circulating particles (see Sec. 3 for a classification of particle orbits). It differs from the well known $2q^2$ factor [19] due to the intrinsic limitation of the ideal MHD model in assuming an isotropic pressure response: $2q^2$ would be the result for $\delta P = \delta P_{\parallel}$, while $\delta P_{\perp} \neq \delta P_{\parallel}$ for the geodesic curvature dynamics in toroidal systems. Similar considerations apply for Eq. (4), where the $\propto 1/q^2$ term is different from $(2q^2)^{-1}$, predicted by ideal MHD [20]. Here, we also note that the shear Alfvén continuum accumulation point ($\Lambda^2 = 0$) given by Eq. (4) is degenerate with the Geodesic Acoustic Mode frequency [20], as pointed out in [21].

Given Eqs. (1) and (2), the mode dispersion relation reads [9, 10]

$$i\Lambda|s| = \delta\hat{W} = \delta\hat{W}_f + \delta\hat{W}_k , \quad (5)$$

where the fluid $\delta\hat{W}_f$, in its simplest expression, is given by [22]

$$\delta\hat{W}_f = 3\pi\Delta q_0 \left(13/144 - \beta_{ps}^2\right) \left(r_s^2/R_0^2\right) \quad (6)$$

with $\beta_{ps} = -(R_0/r_s)^2 \int_0^{r_s} r^2 (d\beta/dr) dr$, R_0 the torus major radius, $\Delta q_0 = 1 - q(r = 0)$ and $\beta = 8\pi P/B_0^2$, the ratio of kinetic and magnetic pressures. The fluid term, $\delta\hat{W}_f$, includes the contribution of the energetic (hot) particle adiabatic and convective responses as well [9]. Meanwhile, the kinetic $\delta\hat{W}_k$ is [9]

$$\delta\hat{W}_k = 4 \frac{\pi^2}{B_0^2} m \omega_c^2 \frac{R_0}{r_s^2} \int_0^{r_s} \frac{r^3}{q} dr \int \mathcal{E} d\mathcal{E} d\lambda \sum_{v_{\parallel}/|v_{\parallel}|=\pm 1} \tau_b \bar{\omega}_d^2 \frac{Q F_0}{\bar{\omega}_d - \omega} , \quad (7)$$

where m is the energetic particle mass, $\omega_c = (eB/mc)$ is the cyclotron frequency, $\mathcal{E} = v^2/2$, $\lambda = \mu B_0/\mathcal{E} = (B_0/B)v_{\perp}^2/v^2$, τ_b is the bounce/transit time for magnetically trapped/circulating particles, ℓ is the arc length along the equilibrium \mathbf{B} -field, $(\dots) = (\oint v_{\parallel}^{-1} d\ell)^{-1} \oint v_{\parallel}^{-1} (\dots) d\ell$ denotes bounce-averaging, ω_d is the magnetic drift frequency and $Q F_0 = (\omega \partial_{\mathcal{E}} + \hat{\omega}_*) F_0$, $\hat{\omega}_* F_0 = \omega_c^{-1} (\mathbf{k} \times \mathbf{B}/B) \cdot \nabla F_0$, with $F_0 = F_0(\mathcal{E}, \lambda, v_{\parallel}/|v_{\parallel}|)$ the fast particle equilibrium distribution function. Here, we also assumed $\Delta q(r) = q(r) - 1 = O(r/R_0)$ [9], but this assumption is easily relaxed. The dispersion relation neglects the thermal ion kinetic response in the ideal region [17], whose analysis is outside the scope of this work and, for our purposes, we can consider as included in the expression of $\delta\hat{W}_f$.

Moving from (\mathcal{E}, λ) to (\mathcal{E}, κ^2) space, with $\kappa^2 = 2(r/R_0)\lambda/[1 - (1 - r/R_0)\lambda]$, $\kappa^2 < 1$ [$0 \leq \lambda < (1 - r/R_0)$] indicates circulating particles, while trapped particles have $\kappa^2 > 1$ [$(1 - r/R_0) < \lambda \leq (1 + r/R_0)$]. Using the (s, α) model tokamak equilibrium [23] ($\alpha = -R_0 q^2 d\beta/dr$), the following expressions for the (bounce, transit) time of (trapped, circulating) particles are obtained:

$$\tau_b^{-1} = \left(\frac{1}{4\mathbb{K}(\kappa)}, \frac{\kappa}{4\mathbb{K}(1/\kappa)} \right) \frac{(2\mathcal{E})^{1/2}}{qR_0} \left[\frac{2(r/R_0)}{2(r/R_0) + (1 - r/R_0)\kappa^2} \right]^{1/2} \quad (8)$$

Here, \mathbb{K} stands for the complete elliptic integral of the first kind. In the same way, the bounce averaged precession frequency $\bar{\omega}_d$ can be computed as [24, 25]:

$$\bar{\omega}_d = \frac{\mathcal{E}}{\omega_c R_0} \frac{\kappa^2(q/r)}{2(r/R_0) + (1 - r/R_0)\kappa^2} \left[1 + \frac{2}{\kappa^2} \left(\frac{\mathbb{E}(\kappa)}{\mathbb{K}(\kappa)} - 1 \right) - \frac{4\alpha}{3\kappa^2} \left(2(1 - 1/\kappa^2) - (1 - 2/\kappa^2) \frac{\mathbb{E}(\kappa)}{\mathbb{K}(\kappa)} \right) - \frac{\alpha}{2q^2} + \frac{4}{\kappa^2} s \left(\frac{\mathbb{E}(\kappa)}{\mathbb{K}(\kappa)} - \frac{\pi}{2\mathbb{K}(\kappa)} (1 - \kappa^2)^{1/2} \right) \right], \quad (9)$$

for circulating particles, whereas, for magnetically trapped particles,

$$\bar{\omega}_d = \frac{\mathcal{E}}{\omega_c R_0} \frac{q}{r} \left[\frac{2\mathbb{E}(1/\kappa)}{\mathbb{K}(1/\kappa)} - 1 + 4s \left(\frac{\mathbb{E}(1/\kappa)}{\mathbb{K}(1/\kappa)} + \frac{1}{\kappa^2} - 1 \right) - \frac{\alpha}{2q^2} - \frac{4\alpha}{3} \left(1 - 1/\kappa^2 + (2/\kappa^2 - 1) \frac{\mathbb{E}(1/\kappa)}{\mathbb{K}(1/\kappa)} \right) \right], \quad (10)$$

where \mathbb{E} stands for the complete elliptic integral of the second kind.

Given Eqs. (3), (4) and (7), Eq. (5) generalizes the electron fishbone dispersion relations, analyzed recently [11, 26], to a broader frequency range as well as to both trapped and barely circulating fast particles, including (s, α) model equilibrium effects on $\bar{\omega}_d$. For the present scope of discussing the electron fishbone excitation by LH only, as on FTU [6, 7], it is necessary to extend Eq. (5) to the case of reversed magnetic shear equilibria [13]. With a simple inertial layer at r_s , with $s = 0$ but finite $S^2 \equiv r_s^2 q_s''/q_s^2$ and $\Delta q \equiv q_s - 1$, the dispersion relation is [13]

$$-S (\Delta q^2 - \Lambda^2)^{3/4} \left[1 + \Delta q / \sqrt{\Delta q^2 - \Lambda^2} \right]^{1/2} = \delta \hat{W}_f + \delta \hat{W}_k. \quad (11)$$

3. Linear excitation of electron fishbones

The crucial features of electron fishbone excitations are dictated by the asymmetry of the shear Alfvén continuum structure at low frequency, quantitatively expressed by Eq. (3), which favors the excitation of modes propagating in the ion diamagnetic direction. Consistently with experimental observations [1, 4, 5], high field side ECRH fulfills this requirement and guarantees both drift-reversal of the barely trapped supra-thermal electrons as well as the inverted spatial gradient of the supra-thermal tail ($\omega_*/\omega > 0$) necessary for effective mode excitation. The case of mode excitation by LH only [6, 7] follows the same physics with few additional twists. The fast electron population which effectively excite the mode are the trapped and barely circulating particles ($\kappa^2 \gtrsim (r/R_0)^{1/2}$), because of Eqs. (7) and (9). Meanwhile, LH power forms a perpendicular fast electron tail, which is moderately slanted towards the counter-current direction;

i.e., despite that it guarantees the inverted spatial gradient of the supra-thermal tail ($\omega_*/\omega > 0$), it is less selective than high field side ECRH in producing particles with drift-reversal. In the case of mode excitation by LH only [6, 7], the presence of circulating supra-thermal particles is crucial for two reasons: (i) barely circulating particles ($\kappa^2 \gtrsim (r/R_0)^{1/2}$) effectively contribute to the mode excitation as described by Eq. (7); (ii) well circulating particles ($\kappa^2 \lesssim (r/R_0)^{1/2}$) modify the current profile, eventually reversing the magnetic shear and broadening the fraction of trapped particles characterized by drift reversal, as shown in Eq. (10). As in the case of ion fishbones, two branches of the electron fishbone exist: a discrete gap mode [10] and a continuum resonant mode [9]. The latter does not generally require neither drift-reversal nor inverted spatial gradient of the supra-thermal tail; however, it has a higher excitation threshold and, thus, it is disfavored, particularly for the branch propagating in the ω_{*e} direction.

Applying Eq. (11) to FTU shot # 20865 (see FIG. 1), the almost steady oscillation of the mode in the low LH power phase and the absence of sawtooth oscillations suggest that $1 \gg \Delta q > 0$. This is consistent with the q -profile reconstruction by transport simulations (FTU has no q profile measurements near the magnetic axis). From experimental observations, $\omega \simeq 60krad/s$, $\omega_{*pi} \simeq 26krad/s$, $\omega_{bi} \simeq 70krad/s$, $\omega_{ti} \simeq 400krad/s$, $\omega_{BAE} \simeq 900krad/s$ and $\omega_A \simeq 9.6Mrad/s$. Thus $\omega_{*pi} < \omega \lesssim \omega_{bi} \ll \omega_{ti}$ and we can apply Eq. (3), showing $\Lambda^2 > 0$. Given the $\omega \lesssim \omega_{bi}$ condition, a further generalization of Eq. (3) would be necessary for a rigorous analysis including mode damping by bounce resonances with thermal ions. These results, however, would simply lead to a redefinition of the mode excitation threshold (see Eq. (14) below) at the expense of technical complications; thus, they will be reported elsewhere. Given Eq. (11), for $\Lambda^2 > \Delta q^2$ the mode can be considered as continuum resonant mode [9], following the standard classification [9]. Assuming $\Delta q \rightarrow 0^+$, for simplicity, the mode dispersion relation becomes

$$\delta\hat{W}_f + \text{Re}\delta\hat{W}_k = (S/\sqrt{2})\Lambda^{3/2} \simeq 0 \quad , \quad (12)$$

which determines the mode frequency [9]; meanwhile, the mode growth rate is defined by [28]

$$\gamma = \Gamma \left[\int_0^{r_s} (r/r_s) (\partial\beta_{h,res}/\partial r) dr - \beta_{h,c} \right] \quad , \quad (13)$$

where $\Gamma = -(R_0/r_s)(\partial\text{Re}\delta\hat{W}_k/\partial\omega)^{-1}$, the effective resonant fast electron normalized pressure, $\beta_{h,res}$, is defined such that $\text{Im}\delta\hat{W}_k \equiv (R_0/r_s^2) \int_0^{r_s} r dr \partial_r \beta_{h,res}$ and the critical excitation threshold $\beta_{h,c}$ is given by

$$\beta_{h,c} = (r_s/R_0)(S/2^{1/2})\Lambda^{3/2} \simeq 1.43(r_s/R_0)^{1/4} S(\omega/\omega_A)^{3/2} (1 - \omega_{*pi}/\omega)^{3/4} \quad . \quad (14)$$

Note that the $\propto \beta_{h,res}$ term in Eq. (13) would change sign for the case of mode excitations by fast ions. With FTU data, $\beta_{h,c}/S \approx 3 \times 10^{-4}$, consistent with the transition observed in FIG. 1, given $\beta_{h,res} \gtrsim 0.7 \times 10^{-4}$ for $P_{LH} = 1MW$ and $\beta_{h,res} \gtrsim 1.2 \times 10^{-4}$ for $P_{LH} = 1.7MW$.

At higher frequencies, $\omega \gg \omega_{ti}$, Eq. (4) applies instead of Eq. (3); thus, the asymmetry of the shear Alfvén continuous spectrum is lost and modes can equally propagate in both ion and electron diamagnetic directions. Equation (4) describes the formation of the Beta induced Alfvén Eigenmodes (BAE) [27] spectral gap: so, electron fishbones propagating in the electron diamagnetic direction and normal pressure profiles could be excited. More precisely, high power ECRH experiments with on axis resonance would be needed, producing sufficiently high effective supra-thermal electron tail temperatures, T_h , for the fast particle precession frequency

to be of the order of the thermal ion transit frequency. For the above FTU parameters, this would require $T_h \gtrsim 200 keV$, to be compared with the usual values $T_h \simeq 30 keV$, as well as $T_e \gg T_i$ for consistency. Note that these fishbones, possibly excited below the BAE frequency, could be equally excited by ICRH induced fast ions but, in that case, they would propagate in the ion diamagnetic direction.

4. Nonlinear amplitude equation

We can generalize Eqs. (5) and (11) closely following the procedure of Ref. [29]. Under the action of the fishbone mode, the toroidally and poloidally symmetric nonlinear modification of the fast electron distribution function is given by

$$\frac{\partial}{\partial t} \delta H_{NL} = -\frac{2}{r} \omega_c \omega^2 \frac{\partial}{\partial r} \left[\left(1 - \frac{(q-1)\bar{v}_{\parallel}}{\omega q R_0} \right) \text{Im} \left(\frac{\bar{\omega}_d}{\bar{\omega}_d - \omega} \right) \left(\frac{Q F_0}{\omega} \right) r^2 r_s^2 |\delta \xi_0|^2 \right]. \quad (15)$$

Here, $\bar{v}_{\parallel} = 0$ for trapped particles and $\delta \xi_0 = \delta \xi_{r0}/r_s$ is the normalized radial displacement of the mode, which is assumed to be the usual step function. Equation (5) can be easily put in the form of a diffusion equation describing the relaxation of the fast particle profile within the $q = 1$ surface:

$$\frac{\partial}{\partial t} n_h = \dot{N}_h - \frac{2}{r} \omega_c \omega^2 \frac{\partial}{\partial r} \left[r^2 r_s^2 |\delta \xi_0|^2 f_{eff,h} \left(\frac{Q_{res} n_h}{\omega} \right) \right]. \quad (16)$$

Here, \dot{N}_h indicates the fast electron source term due to additional power input, we have defined the effective fraction of fast electrons $f_{eff,h}$ and

$$f_{eff,h} \left(\frac{Q_{res} n_h}{\omega} \right) = \langle F_0 \rangle^{-1} \left\langle \left(1 - \frac{(q-1)\bar{v}_{\parallel}}{\omega q R_0} \right) \text{Im} \left(\frac{\bar{\omega}_d}{\bar{\omega}_d - \omega} \right) \left(\frac{Q F_0}{\omega} \right) \right\rangle, \quad (17)$$

having indicated velocity space integration by angular brackets. From Eqs. (16) and (17) we recognize that the nonlinear diffusion coefficient due to the fishbone within the $q = 1$ surface is given by $D_{NL} \simeq 2\omega r_s^2 f_{eff,h} |\delta \xi_0|^2$. Using Eq. (15), meanwhile, the nonlinear modification for the resonant contribution (imaginary part) of $\delta \hat{W}_k$ is obtained in the form:

$$\begin{aligned} |\delta \xi_0|^{-2} \frac{\partial}{\partial t} \left[\left(\frac{\partial}{\partial t} \delta \hat{W}_{k,NL} \right) |\delta \xi_0|^2 \right] &\simeq -8i \frac{\pi^2}{B_0^2} m \omega_c^3 \omega^2 \frac{R_0}{r_s^2} \int_0^{r_s} \frac{r^2}{q} dr \int \mathcal{E} d\mathcal{E} d\lambda \\ &\times \sum_{v_{\parallel}/|v_{\parallel}|=\pm 1} \tau_b \bar{\omega}_d^2 \text{Im} \left(\frac{Q}{\bar{\omega}_d - \omega} \right) \frac{\partial}{\partial r} \left[r^2 r_s^2 Q F_0 \left(1 - \frac{(q-1)\bar{v}_{\parallel}}{\omega q R_0} \right) |\delta \xi_0|^2 \right]. \end{aligned} \quad (18)$$

That $\delta \hat{W}_{k,NL}$ is predominantly imaginary, suggests that the real frequency of the fishbone mode in the nonlinear regime is still given by an equation in the form of Eq. (12): i.e., the mode frequency is expected to *chirp* downward as the fast particles relax, according to Eq. (16). More specifically, the nonlinear evolution equation for the real frequency is

$$\delta \hat{W}_f + \text{Re} \delta \hat{W}_k + \text{Re} \delta \hat{W}_{k,NL} = (S/\sqrt{2}) \Lambda^{3/2} \simeq 0. \quad (19)$$

Giving the exact expression of $\text{Re} \delta \hat{W}_{k,NL}$ is beyond the scope of the present paper. Here, we simply note that the nonlinear time scale in Eq. (19) is $\propto |\delta \xi_0|^{-2}$, consistent with Eq. (16). Meanwhile, the amplitude evolution equation can be formally written as Eq. (13),

$$(d/dt) |\delta \xi_0|^2 = 2\Gamma \left[\int_0^{r_s} (r/r_s) (\partial \beta_{h,res}/\partial r) dr - \beta_{h,c} \right] |\delta \xi_0|^2, \quad (20)$$

where the nonlinear evolution equation for the resonant fast particle pressure gradient becomes

$$\frac{\partial}{\partial t} \left[|\delta\xi_0|^2 \left(\frac{\partial}{\partial t} - \nu_{ext} \right) \frac{\partial}{\partial r} \beta_{h,res} \right] = 2C\omega^2 \frac{r_s^2}{r^2} |\delta\xi_0|^4 \frac{\partial^2}{\partial r^2} \left(r^2 \frac{\partial}{\partial r} \beta_{h,res} \right) . \quad (21)$$

Here, ν_{ext} is the reconstruction rate of $\beta_{h,res}$, i.e.,

$$\nu_{ext} = 4 \frac{\pi^2}{B_0^2} \frac{m\omega_c}{\partial_r \beta_{h,res}} \frac{r^2 k_\theta}{q} \int \mathcal{E} d\mathcal{E} d\lambda \sum_{v_\parallel/|v_\parallel|=\pm 1} \text{Im} \left(\frac{\tau_b \bar{\omega}_d^2}{\bar{\omega}_d - \omega} \right) \frac{\partial}{\partial r} \frac{\partial}{\partial t} F_{0,ext} , \quad (22)$$

where $\partial_t F_{0,ext}$ is the rate of change of the fast particle distribution function due to external sources (inclusive of Coulomb collisions); meanwhile, C is a constant of order unity which may be computed exactly, given Eq. (18) the definition of $\beta_{h,res}$.

Equations (20) and (21) are a simple model which fully describes the fishbone cycle due to quasilinear wave-particle resonances. This formal analysis, thus, is equivalent in spirit to the approach of [30] and the numerical analysis of [31], but has the advantage of treating explicitly the energetic particle nonlinear dynamics. The nonlinear time scale, τ_{NL} , as derived from Eq. (21), scales as $(2C)^{1/2} \omega \tau_{NL} \approx |\delta\xi_0|^{-1}$, consistent with the predator-prey model for the fishbone cycle proposed in [9] and in contrast with the time scale $\propto |\delta\xi_0|^{-2}$ of Eq. (19). This is a consequence of the fundamental role of resonant particles in the fishbone dynamics and of the more efficient wave-particle scattering out of the resonance region. Detailed analyses of Eqs. (20) and (21) will be reported elsewhere, along with comparisons with FTU experimental observations.

5. Discussions and conclusions

In this work, we have analyzed the excitation of electron fishbones by both trapped as well as barely circulating supra-thermal electrons, providing a unified explanation of the various experimental observation of these modes. The possibility of exciting fishbone modes at frequencies just below the BAE accumulation point by both fast electrons and ions is also discussed.

The most interesting feature of electron fishbones is their relevance to burning plasmas. In fact, unlike fast ions in present day experiments, fast electrons are characterized by small orbits, which do not introduce additional complications in the physics due to nonlocal behaviors, similarly to alpha particles in reactor relevant conditions. Meanwhile, the bounce averaged dynamics of both trapped as well as barely circulating electrons depends on energy (not mass): thus, their effect on low frequency MHD modes can be used to simulate/analyze the analogous effect of charged fusion products. Furthermore, the combined use of ECRH and LH provide extremely flexible tools to investigate various nonlinear behaviors, of which FTU experimental results provide a nice and clear example (see Figure 1).

Acknowledgments

The authors are indebted to useful and stimulating discussions with J.P. Graves and R.J. Hastie. This work was supported by the Euratom Communities under the contract of Association between EURATOM/ENEA. This work was also supported by the U.S. DOE Contract No. DE-AC02-CHO-3073.

- [1] WONG, K.L., et al., Phys. Rev. Lett. **85** (2000) 996
- [2] VALOVIC, M., et al., Nucl. Fusion **40** (2000) 1569
- [3] CHENG, C.Z., CHEN, L., and CHANCE, M.S., Ann. Phys. (1985) **161** 21
- [4] DING, X.T., et al., Nucl. Fusion **42** (2002) 491
- [5] LI, J., et al., “High Performance Discharges in the HT-7 and HL-1M Tokamaks”, Fusion Energy 2002 (Proc. 19th Int. Conf. Lyon, 2002), C&S Papers Series No. 19/C, IAEA, Vienna (2003), CD-ROM file Ov/5-1 and <http://www.iaea.org/programmes/ripc/physics/fec2002/html/fec2002.htm>
- [6] SMEULDERS, P., et al., “Fast MHD Analysis on FTU”, (Proc. 29th EPS Conf. on Pl. Phys. Contr. Fus. Montreux, 2002), Eur. Conf. Abs. **26B** (2002) D-5.016 and <http://epsppd.epfl.ch/Montreux/start.htm>
- [7] ROMANELLI, F., et al., “Overview of the FTU Results”, Fusion Energy 2002 (Proc. 19th Int. Conf. Lyon, 2002), C&S Papers Series No. 19/C, IAEA, Vienna (2003), CD-ROM file Ov/4-5 and <http://www.iaea.org/programmes/ripc/physics/fec2002/html/fec2002.htm>
- [8] MCGUIRE, K., et al., Phys. Rev. Lett. **50** (1983) 891
- [9] CHEN, L., WHITE, R.B., and ROSENBLUTH, M.N., Phys. Rev. Lett. **52** (1984) 1122
- [10] COPPI, B., and PORCELLI, F., Phys. Rev. Lett. **57** (1986) 2272
- [11] WANG, Z.T., et al., Chin. Phys. Lett. **23** (2006) 158
- [12] ZONCA, F., and CHEN, L., Plasma Phys. Control. Fusion **48** (2006) 537
- [13] HASTIE, R.J., et al., Phys. Fluids **30** (1987) 1756
- [14] COPPI, B., GREENE, J.M., and JOHNSON, J.L., Nucl. Fusion **6** (1966) 101
- [15] PEGORARO, F., and SCHEP, T.J., Plasma Phys. Control. Fusion **28** (1986) 647
- [16] MIKHAILOWSKII, A.B., and TSYPIN, V.S., Sov. J. Plasma Phys. **9** (1983) 91
- [17] GRAVES, J.P., et al., Plasma Phys. Control. Fusion **42** (2000) 1049
- [18] ZONCA, F., et al., Plasma Phys. Control. Fusion **38** (1996) 2011
- [19] GLASSER, A.H., GREEN, J.M., and JOHNSON, J.L., Phys. Fluids **18** (1975) 875
- [20] WINSOR, N., JOHNSON, J.L., and DAWSON, J.M., Phys. Fluids **11** (1968) 2448
- [21] ZONCA, F., BRIGUGLIO, S., CHEN, L., FOGACCIA, G., HAHM, T.S., MILOVANOV, A.V., and VLAD, G., “Physics of Burning Plasmas in Toroidal Magnetic Confinement Devices” (submitted to Plasma Phys. Control. Fusion)
- [22] BUSSAC, M.N., et al., Phys. Rev. Lett. **35** (1975) 1638
- [23] CONNOR, J.W., HASTIE, R.J., and TAYLOR, J.B., Phys. Rev. Lett. **40** (1978) 396
- [24] ROSENBLUTH, M., and SLOAN, M.L., Phys. Fluids **14** (1971) 1725
- [25] CONNOR, J.W., HASTIE, R.J., and MARTIN, T.J., Nucl. Fusion **23** (1983) 1702
- [26] SUN, Y.W., et al., Phys. Plasmas **12** (2005) 092507
- [27] HEIDBRINK, W.W., et al., Phys. Rev. Lett. **71** (1993) 855
- [28] WHITE, R.B., ROMANELLI, F., and BUSSAC, M.N., Phys. Fluids B **2** (1990) 745
- [29] ZONCA, F., et al., Nucl. Fusion **45** (2005) 477
- [30] BREIZMAN, B.N., et al., Phys. Plasmas **5** (1998) 2326
- [31] CANDY, J., et al., Phys. Plasmas **6** (1999) 1822